Object localization in seawater via electrical impedance measurements

Arthur-Vincent Lindenberg*, Gunther Ardelt*, Fabian John* and Horst Hellbrück*
* Luebeck University of Applied Sciences, Germany
Department of Electrical Engineering and Computer Science
Email: arthur@lindenberg-online.com, gunther.ardelt@th-luebeck.de, fabian.john@th-luebeck.de horst.hellbrueck@th-luebeck.de

***Abstract*—Artificial technical infrastructures already exist on and in the seabed, including cables for energy and data communication and pipelines for oil and gas. There are also contaminated sites such as blind munitions, which can contaminate the sea and which can hinder the development of new infrastructures. Objects such as blind ammunition, mines and barrels should be discovered and removed in order to avoid damage to people and the environment. Deep-sea cables and pipelines are regularly checked for their laying depth, for example, which can change due to currents. One approach to the tracking of cables, the detection and localization of metal objects is electrical impedance spectroscopy and tomography. The first results of this approach are presented here, which were achieved with a test stand in which impedance measurements in salt water are reproducible under laboratory conditions. With the test stand variable objects can be varied in their position in space in relation to a static electrode array. The results show the horizontal and vertical sensitivity of an electrode array for different dimensions of objects, based on the measured impedance. A simple algorithm that uses previously measured impedances in the form of a look-up table basically shows the successful detection and localization of objects in the vicinity of the array.**

***Index Terms*—electrical impedance, object detection and localization in seawater, cable tracking.**

I. Introduction

In the past many remains of wars and other debris have been dumped in the oceans. Ammunition and barrels containing toxic waste are meant to be never found again. For protection of life and to ensure a sustainable environment those objects should be localized and collected. Almost all of these objects have a metal surface. An auspicious beginning is to test for electrical conductivity. In addition, numerous deep-sea cables for power supply and telecommunications are being laid in the oceans today. For maintenance purposes the cables have to be located again. Even when cables position are documented during installation, the positions can change due to the tide and fishing. In terms of electrical conductivity, these shielded cables present themselves as non-conductors compared to the surrounding seawater. The EXTENSE project of the CoSA competence center is dedicated to the search for efficient detection methods to find underwater objects, especially deep-sea cables. One of the projects approaches is a electrical impedance based measurement system. The long term goal is to mount the system on a marine vessel and test it under real conditions. As a prerequisite, a small test stand must be examined under laboratory conditions.

The contributions of this paper are:

- Measurement series to asses the test stand
- Evaluation of horizontal and vertical sensitivity
- Localisation of a metal object

II. Related Work

A number of methods for underwater object detection with different use cases are known. The typical approach for general object detection is to use sonar sensing, but interpreting sonar images is quite difficult for small objects [1]. Another approach by Buchette [2] is in the use of electrical impedance tomography (EIT), which works in proximity but introduces the mathematical complex forward problem and inverse problem [3]. Preliminary investigations about impedance measurement have also been made by Schuldei et al. [4]. The measurement range could theoretical be improved compared to EIT, and it does not require a solution to the mathematical problems.

Xu [5] introduces specialized underwater cable shape detection methods and describes the benefits and drawbacks of different measurement systems. Underwater cable tracking systems by active pulse induction, which are presented by Cowls [6] can only cover short distances and have to be calibrated for several parameters.

Furthermore, there are systems to detect current carrying cables. Schuldei [4] describes the use of passive induction detection from Tinsley company, but it varies greatly in accuracy and depends on an experienced operator.

The measurement systems for underwater object detection still have limited use cases and disadvantages. Therefore, an EIT-inspired approach to impedance measurement is investigated in more detail using a newly developed test stand.

III. Idea

The objective of this publication is to investigate impedance changes in seawater through a metal object using a test stand. At the beginning, the setup of the experiment is presented. The following figure 1 shows a photograph of the measurement setup. Here an aquarium filled with salt water and a layer of sediment is shown. Above the sediment layer, there is an arrangement of transmitting and receiving electrodes, which is referred to below as the electrode array. The metal object for this test case is an aluminum cylinder with a length of 12,5 cm and a diameter of 5 cm. This aluminum cylinder is hung up to change the electrical conductivity of the salt water in the aquarium. Because of the size of electrode array it can not be moved. So instead the the metal object is moved above the electrode array remotely via a construction of stepper motors. This construction is called the XY-table in the following.

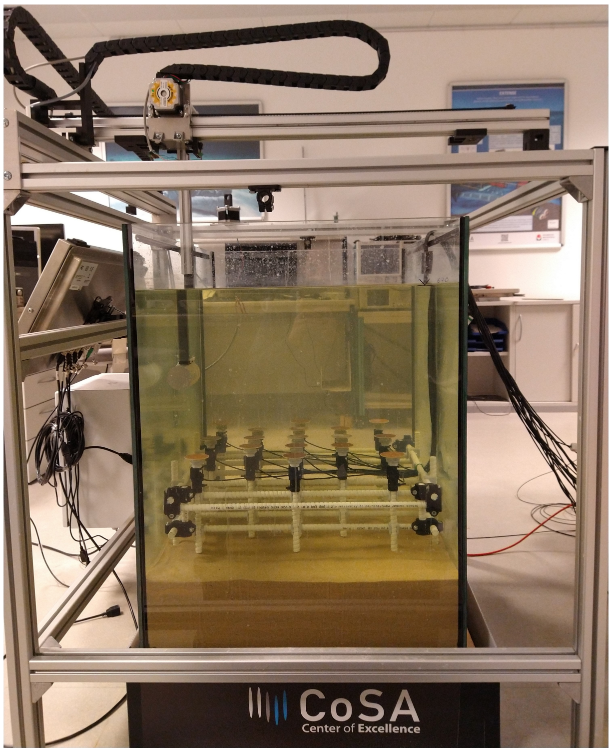

Fig. 1. Experimental setup of aquarium, electrode array, XY-table and measuring object

In the next step, the measurement setup is explained in more detail using a block diagram. The figure 2 shows the simplified structure of the overall system for a single pair of electrodes. A sinusoidal voltage is first generated using a frequency generator. A voltage-controlled current source (VCCS) generates a measurement current from this. The measuring current is impressed on a pair of transmitting electrodes (dipole) in the aquarium. The voltage drop between a receiving electrode and a reference electrode is recorded. The electrode array contains 8 of these receiving electrodes and 4 transmitting dipoles. The voltages are picked up by the receiving electrodes using an ADC card in a PC. A MATLAB program controls the voltage-controlled current source, the ADC card, the XY position of the aluminum cylinder and saves the measured values. Impedances are then calculated from the impressed currents and the measured voltage drops.

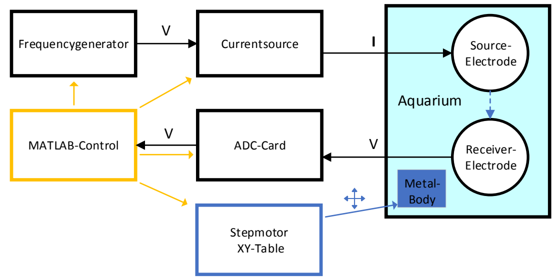

Fig. 2. Block diagram of the experiment setup

In the next section the exact arrangement of the experimental setup shown in Figure 1 is explained.

IV. Implementation

The figure 3 describes the experimental setup inside the aquarium in top view. It shows the axis arrangement of the test setup, which is kept consistent across all graphics. All electrodes have a diameter of 5 cm. The 9 inner electrodes have a vertical and horizontal distance of 10 cm from one another. While the outer 8 electrodes are spaced 20 cm apart. The electrode array is placed in an axisymmetrical manner on the sediment in the center of the aquarium. The aluminum cylinder has a length of 12.5 cm and a diameter of 5 cm.

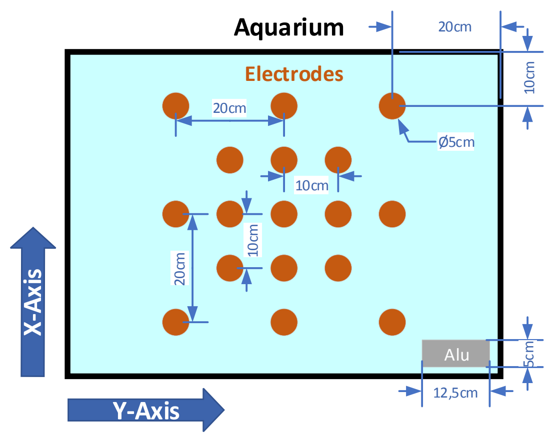

Fig. 3. Experimental setup of aquarium and electrode array

The next figure 4 shows the connection of the electrodes in the electrode array. The transmitting electrodes for feeding the current are labeled with the letter (S) for send. The blue arrows show the sending dipoles which consist of a pair of transmitting electrodes. The receiving electrodes are marked with the letter (R) for receive and are connected to the reference electrode (REF) in the center. Here indicated by the black arrows.

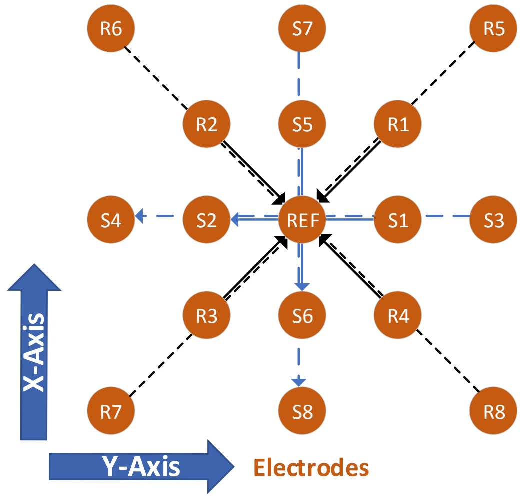

Fig. 4. Experimental arrangement of the transmitter and receiver electrodes in the electrode array

A series of measurements is carried out using the test setup described. With the stepper motors of the XY table, the aluminum cylinder is moved 4 cm on the X axis in the interval from 0 cm to 48 cm. There is a further movement along the Y-axis from 0 cm to 60 cm, also in 4 cm steps. This results in a plane area (z-position) with 13 x-positions $\times$ 16 y-positions $=$ 208 measuring positions. A total of 8 such areas are recorded at 4 cm intervals at a vertical distance of 2 cm to 30 cm from the electrode array. At each individual measuring positions, sinusoidal currents of 100 mA at three different frequencies of 10 kHz, 50 kHz and 100 kHz are fed in successively via the 4 dipole pairs from Figure 4. For each transmitting dipole, the voltage drops at the 8 receiving electrodes are measured. In addition, the current curves of the 4 transmission dipoles are measured via a shunt resistor for each measuring point. Thus for each measuring point of an area there are 4 sending dipoles $\times$ 8 receiving electrodes $\times$ 3 frequencies $=$ 96 values of voltage curves recorded.

In the following evaluation, the stimulating frequency of 10 kHz is always considered in order to save at least one of the 6 dimensions (x-position, y-position, z-position, receiving electrode, transmission dipole, frequency).

V. Evaluation

First, the voltage and current curves recorded for the individual measuring points are transformed into the spectral range using FFT [7]. According to the equations 1 and 2 the magnitude and phase of the impedance spectrum are formed.

$$|Z(\omega)| = \frac{|U(\omega)|}{|I(\omega)|} \tag{1}$$

$$\phi = \arctan \frac{|U(\omega)|}{|I(\omega)|} \tag{2}$$

In addition to the desired determination of the change in impedance in salt water due to the presence of a metal object, there is also a considerable reduction in data.

In the next steps, the measurement results of this test setup are examined for vertical and horizontal sensitivity. The position of the aluminium sensor is also determined with the help of a look-up algorithm.

A. Vertical sensitivity

The table I shows the maximum changes in the impedances in magnitude and phase for entire measuring areas (z-positions). All 8 receiving electrodes and the 4 transmission dipoles are taken into account for this calculation. Here it becomes visible that after large changes for the first two areas, the changes from area 3 onwards remain almost constant.

Areas	*Max.* $Z(\omega)$ *in* Ω	*Max.* ϕ *in degree*
1	3.276	1.254
2	1.453	0.510
3	1.261	0.437
4	1.254	0.432
5	1.255	0.433
6	1.255	0.435
7	1.262	0.437
8	1.263	0.437

TABLE I
MAXIMAL MAGNITUDE AND PHASE CHANGES OVER THE AREAS.

The next step is a more detailed evaluation of the maximum change in the magnitude of the impedance using the illustration 5. All 8 electrodes are taken into account in this calculation and the 4 dipoles are plotted over the areas. A comparison with Table 1 above shows that the maximum impedance of area 1 comes from dipole 1-2 and all other contributions in table 1 are from dipole 5-6.

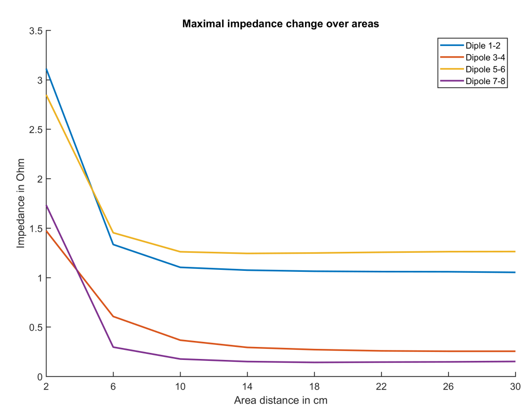

Fig. 5. Maximum change in impedance for 4 dipoles over the distance of the 8 measuring areas; Frequency = 10 kHz

The figure 6 goes into more detail and shows the 8 receiving electrodes over 5 areas for each dipole next to each other. The change in the magnitude of impedances is also evaluated, but with the logarithm of the Y-axis. All curves are fairly similar to each other. The largest deviation in the impedances among the 8 electrodes takes place when current is fed by means of dipoles 7-8.

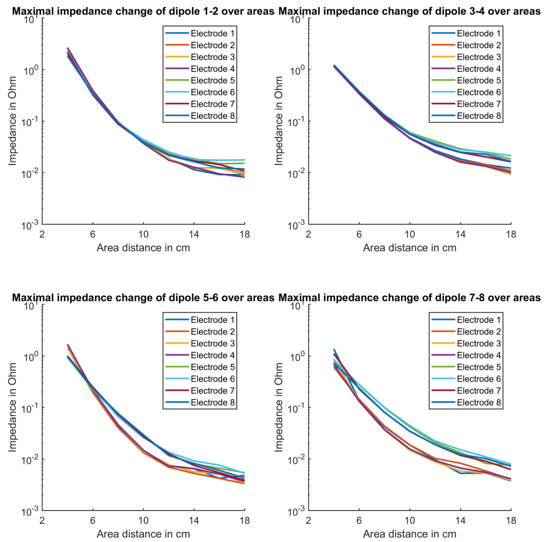

Fig. 6. Maximum change in impedance of 8 electrodes over the distance of 5 measuring areas for 4 dipoles; Logarithm of the Y-axis; Frequency = 10 kHz

The figure 7 shows the same processing of the measurement data as the previous figure 6. But here the maximal change of the phase angle is plotted. The course of the phase change has a slight deviation from the course of the impedance change. The inner four electrodes form a group with a faster decrease in phase change compared to the outer electrodes.

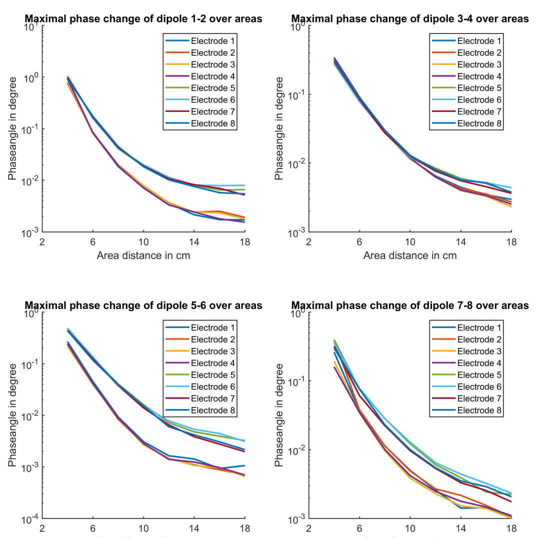

Fig. 7. Maximum change in the phase angle of 8 electrodes over the distance of 5 measuring planes for 4 dipoles; Logarithm of the Y-axis; Frequency = 10 kHz

B. Horizontal sensitivity

To illustrate the sensitivity in the horizontal direction, the electrode 1 is shown as an example in different areas of the measurement series. All impedances shown in the following figures are normalized to values between 0 and 1.

The figure 8 shows the change in the magnitude of the impedance for 4 areas at distances of the electrode array from 2 cm to 26 cm. The receiving electrode is fed by dipole 1-2. Minima are represented in a dark blue colour, while maxima are light yellow. It can be seen that the minima on the surface with the smallest distance to the aluminium cylinder are spatially sharply defined. However, with increasing vertical distance from the aluminum object, the measurement result becomes less precise in horizontal direction.

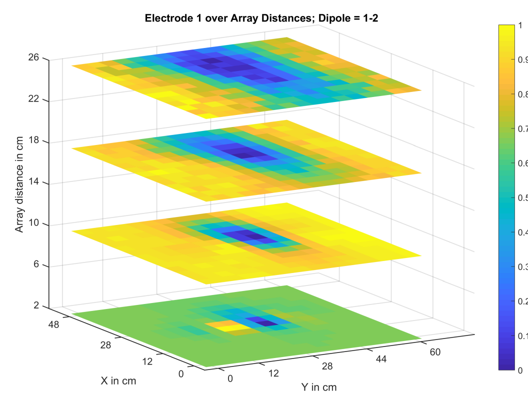

Fig. 8. Electrode 1 when current is impressed via dipole 1-2; Vertical distance from the electrode array = 2 cm to 26 cm; Frequency = 10 kHz

In figure 9 the electrode 1 is shown again with planes identical to the previous figure 8. The difference lies in the injection of a current through the dipole 5-6. Here the top area is very noisy and minimum in the bottom area almost invisible. A more detailed view is presented in the next section.

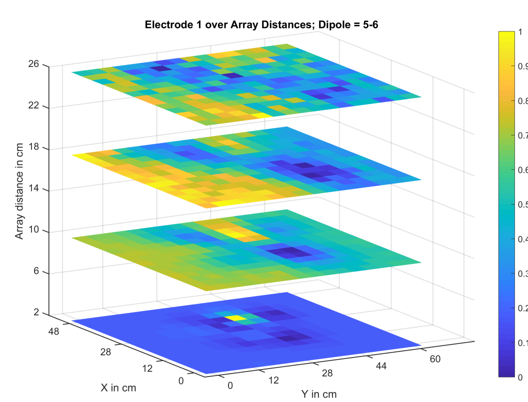

Fig. 9. Electrode 1 when current is impressed via dipole 5-6; Vertical distance from the electrode array = 2 cm to 26 cm; Frequency = 10 kHz

C. Evaluation of individual electrodes

The illustration 10 shows the color processed picture of the area with a distance of 10 cm to the metal object. The magnitude of the impedance over receiving electrode 1 is shown for the feed over all four dipoles. To indicate the receiving electrode 1 a red circle is used, and its reference electrode in the center is a green colored circle. The transmission dipole electrodes are blue colored circles. This colourisation is also used for the following pictures. The minima appear in blue and are located between the measurement electrode and the reference when current feed is supplied via dipole 1-2 and dipole 3-4. The coordinates of the minima while current feed is supplied via dipole 5-6 and dipole 7-8 differ considerably from one another.

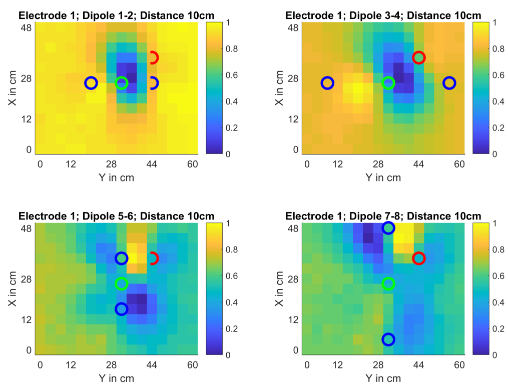

Fig. 10. Electrode 1 with current injection via 4 dipoles; Vertical distance from the electrode array = 10 cm; Frequency 10 kHz

The figure 11 shows the magnitude of the impedances in one area for the four inner electrodes 1 to 4 with a current feed via dipole 1-2. All minima are located between receiving electrodes and the reference electrode. This effect could provide information for further localization.

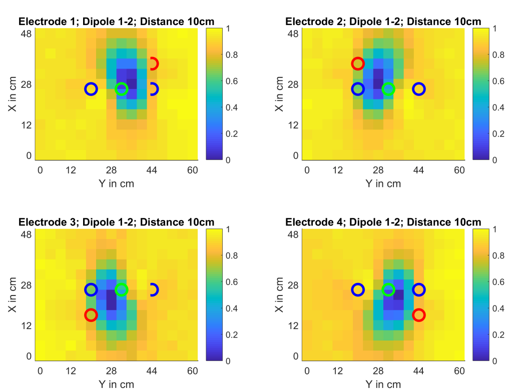

Fig. 11. Electrodes 1 to 4 with current injection via dipole 1-2; Vertical distance from the electrode array = 10 cm; Frequency 10 kHz

The figure 12 shows the magnitude of impedances in one area for the four inner electrodes 1 to 4 when power is fed via dipole 5-6. Instead of a minimum at the corresponding positions in the electrode array from Figure 4, a maximum appears in its vicinity.

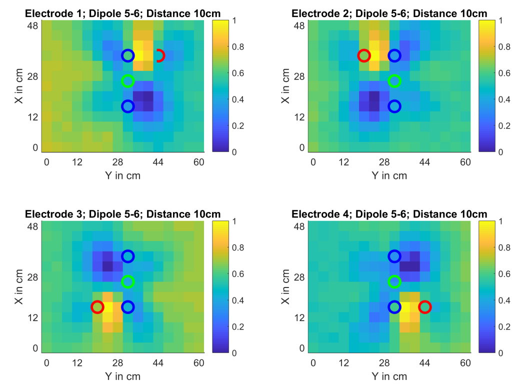

Fig. 12. Electrodes 1 to 4 when current is impressed via dipole 5-6; Vertical distance from the electrode array = 10 cm; Frequency = 10 kHz

D. Evaluation of the horizontal position of the aluminum object

In the following figures, the magnitudes of impedances are plotted against the electrode positions for a selected measuring point. The image 4 is used as base of the model. The corresponding electrode positions are placed over a image matrix designed for this purpose. The smallest value or a dark blue color stands for the assumed position of the aluminum cylinder in the image matrix.

The figure 13 shows the magnitude of impedance at the measuring point X = 24 cm and Y = 40 cm with an excitation by dipole 1-2. The assumed horizontal position is close to receiving electrode 1.

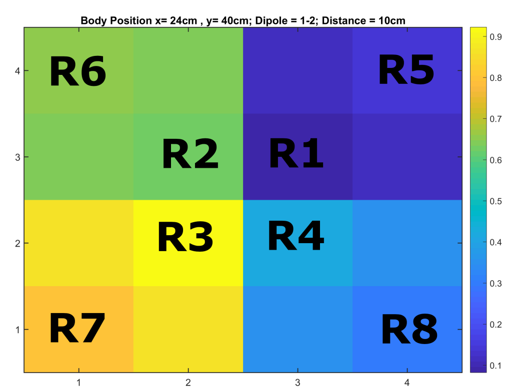

Fig. 13. Measuring object position at coordinate X = 24 cm and Y = 40 cm with current impression by means of dipole 1-2; Vertical distance from the electrode array = 10 cm; Frequency 10 kHz

The figure 14 shows the magnitude impedance at the same measuring point X = 24 cm and Y = 40 cm but with an excitation by dipole 3-4. The assumed horizontal position is again close to receiving electrode 1.

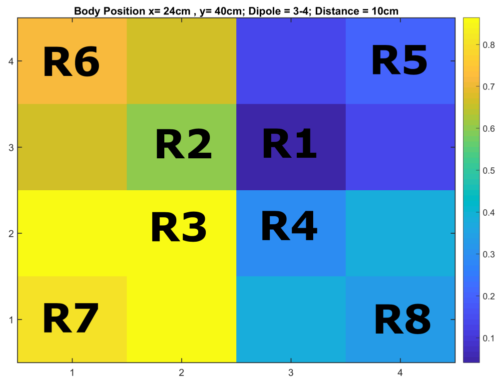

Fig. 14. Measuring object position at coordinate X = 24 cm and Y = 40 cm with current impression by means of dipole 3-4; Vertical distance from the electrode array = 10 cm; Frequency 10 kHz

The figure 15 shows again the magnitude of impedance at measuring point X = 24 cm and Y = 40 cm but now with an addition of the impedances and subsequent normalization by dipoles 1-2 and 3-4. The assumed position stays close to receiving electrode 1.

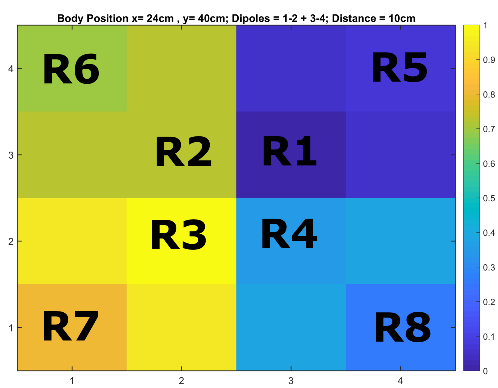

Fig. 15. Measuring object position at coordinate X = 24 cm and Y = 40 cm with current feed by dipoles 1-2 and 3-4; Vertical distance from the electrode array = 10 cm; Frequency = 10 kHz

Now another measurement point is used with the same addition of impedances from the last figure. The figure 16 shows the magnitude of impedance at measuring point X = 16 cm and Y = 28 cm with an added excitation by dipoles 1-2 and 3-4. The assumed position is now in vicinity to the receiving electrode 6.

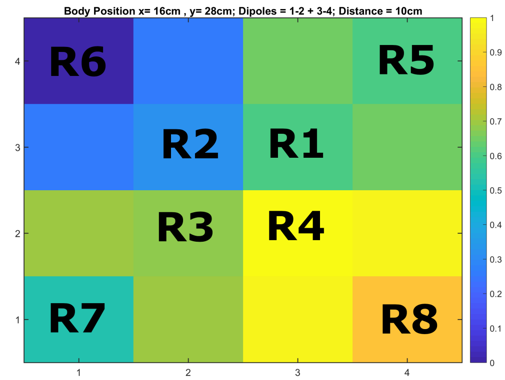

Fig. 16. Measuring object position at coordinate X = 16 cm and Y = 28 cm with current feed by dipoles 1-2 and 3-4; Vertical distance from the electrode array = 10 cm; Frequency = 10 kHz

A last measurement point in the bottom left corner of the aquarium is used. The figure 17 shows the magnitude of impedance at measuring point X = 12 cm and Y = 12 cm with an added excitation by dipoles 1-2 and 3-4. Now the detection of the position becomes less clear because of a chosen measurement point outside of the electrode array. The it is assumed that the closest electrode in number 7.

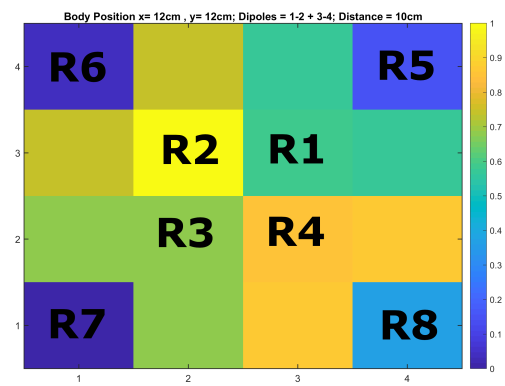

Fig. 17. Measuring object position at coordinate X = 12 cm and Y = 12 cm with current feed by dipoles 1-2 and 3-4; Vertical distance from the electrode array = 10 cm; Frequency = 10 kHz

VI. Conclusion and Future Work

In the case of close proximity to a receiving electrode, the position of the aluminum cylinder can be clearly determined with the look-up algorithm introduced in the last part. When the aluminium cylinder is not above the array the horizontal position becomes uncertain. More objects with different sizes and materials should also be tested in the near future.

In addition, it can be seen that the sensitivity of the measurement decreases rapidly with increasing distance from the measuring object, both vertically and horizontally. However, this is a test setup that has been greatly reduced in size to reality. An electrode array would have a diameter of several square meters on the high seas. The applied current is also limited in this structure and the aluminum cylinder used is comparatively short to mine or even a deep sea cable. Further tests under real conditions are therefore necessary for a final judgment on this measurement method for metal object detection.

Acknowledgments

This publication is a result of the research of the Center of Excellence CoSA and funded by the Federal Ministry of Education & Research of the Federal Republic of Germany (Id [03SX467B], [EXTENSE]). Horst Hellbrück is adjunct professor at the Institute of Telematics of University of Lübeck.

References

[1] M. Valdenegro-Toro, “Submerged marine debris detection with autonomous underwater vehicles,” in *2016 International Conference on Robotics and Automation for Humanitarian Applications (RAHA)*. IEEE, dec 2016.

[2] G. Bouchette, P. Church, J. E. Mcfee, and A. Adler, “Imaging of compact objects buried in underwater sediments using electrical impedance tomography,” *IEEE Transactions on Geoscience and Remote Sensing*, vol. 52, no. 2, pp. 1407–1417, feb 2014.

[3] P. M. Faia, R. Silva, M. G. Rasteiro, F. A. P. Garcia, A. R. Ferreira, M. J. Santos, J. B. Santos, and A. P. Coimbra, “Imaging particulate two-phase flow in liquid suspensions with electric impedance tomography,” *Particulate Science and Technology*, vol. 30, no. 4, pp. 329–342, jul 2012.

[4] A. Schuldei, T. Suthau, F. John, G. Ardelt, and H. Hellbruck, “Development of an electro impedance tomography-based platform for measurement of burial depth of cables in subsea sediments,” in *OCEANS 2019 - Marseille*. IEEE, jun 2019.

[5] C. Xu, J. Chen, D. Yan, and J. Ji, “Review of underwater cable shape detection,” *Journal of Atmospheric and Oceanic Technology*, vol. 33, no. 3, pp. 597–606, mar 2016.

[6] S. Cowls and S. Jordan, “The enhancement and verification of a pulse induction based buried pipe and cable survey system,” in *OCEANS ’02 MTS/IEEE*, vol. 1, 2002, pp. 508–511 vol.1.

[7] S. Kaufmann, “Instrumentierung der bioimpedanzmessung,” Ph.D. dissertation, Universität zu Lübeck, 2015.